[AMERICAN JOURNAL OF SCIENCE, VOL. 293, APRIL, 1993, P. 257–296]

American Journal of Science

APRIL 1993

SCALING PROPERTIES OF TIME-SPACE KINETIC MASS TRANSPORT EQUATIONS AND THE LOCAL EQUILIBRIUM LIMIT

Peter C. Lichtner*

Hydrochemie Gruppe, Geologisches und
Mineralogisch-petrographisches Institut, Universität Bern,
Baltzer-Strasse 1, CH-3012 Bern, Switzerland

ABSTRACT. Scaling properties of kinetic mass conservation equations are presented, and their implications investigated for advective and diffusive transport in an isothermal system in a single spatial dimension. It is demonstrated that for a system undergoing pure advection, scaling the kinetic rate constants by a common factor, thereby preserving their ratios, is equivalent to scaling the time and space coordinates of the original solution. Diffusive transport requires that the diffusion coefficient must also be scaled by the reciprocal factor. These results have far reaching consequences on the possible form of solutions of the kinetic mass transport equations. It follows that the local equilibrium solution, corresponding to the limit as the kinetic rate constants approach infinity, can be extracted from a solution belonging to finite rate constants merely by scaling the time and space coordinates of the kinetic solution. Furthermore the velocities of boundaries of mineral reaction zones must approach their local equilibrium counterparts with increasing time. As a practical consequence, numerical solutions to differential equations representing fluid transport and kinetic reactions of minerals can be validated against solutions to algebraic equations representing conditions of local equilibrium for pure advective transport. Such a test is especially important when attempting to predict the consequences of processes evolving over geologic time spans. The theory is illustrated for a single component system for which an analytical solution exists. A numerical example of weathering is presented for which kinetic and local equilibrium solutions are compared. Finally it is suggested that the recent controversy regarding the discrepancy between laboratory and field derived kinetic rate constants may be a consequence of neglect of the affinity factor in the expression for the reaction rate when applied to field observations. This error can lead to field rate constants that are too small by several orders of magnitude.

* Present address: Southwest Research Institute, Center for Nuclear Waste Regulatory Analyses; 6220 Culebra Road, San Antonio, Texas 78228-0510.

LIST OF SYMBOLS

A_i^{rev}	designation for the ith reversibly reacting aqueous complex.
A_j	designation for the jth primary species.
$\mathbf{A}_m$	affinity of the mth mineral.
$\mathbf{A}_m^{th}$	threshold affinity for the onset of precipitation of the mth mineral.
a	general scale factor applied to the space coordinate.
b	general scale factor applied to the time coordinate.
C_{eq}	equilibrium concentration.
C_i	concentration of the ith reversibly reacting aqueous complex.
C_j	concentration of the jth primary species.
C_l	concentration evaluated at the reaction front l(t).
$C_\pm$	concentration on the downstream and upstream sides of the reaction front for the single component system.
C	solute concentration in the single component system.
C_0	inlet concentration in the single component system.
C_∞	initial concentration in the single component system.
D	diffusion coefficient.
erfc(x)	complementary error function.
F(x, t)	notation for a general function of time and space coordinates.
$f_{\sigma(x,\,t)}$	scaled function f.
F(x, t; {k}, D, u)	general designation for a field variable representing solute concentration or mineral volume fraction.
I_m	net reaction rate of the mth mineral.
K_m	equilibrium constant corresponding to the overall reaction of the mth mineral.
k_m	kinetic rate constant associated with the overall reaction of the mth mineral.
k	kinetic rate constant in the single component system.
{k}	collective set of kinetic rate constants $\{k_1; \ldots; k_M\}$.
K_Δ	distribution coefficient between solid and aqueous phases.
l(t)	reaction front position.
l_m; $l_m^{(i)}$	reaction front corresponding to the mth mineral (for the ith zone boundary).
$\mathscr{M}_m$	designation for the mth mineral.
M	number of reacting minerals.
N	number of primary species.
n_m	number of moles of the mth mineral in a closed system.
Q_m	ion activity product corresponding to the mth mineral.
q	inverse length characterizing the distance for the solute concentration to reach equilibrium.
R	gas constant.

s_m	surface area of the mth mineral per unit volume of bulk rock.
s	solid surface area per unit volume of bulk rock in the single component system.
$T(x, t)$	temperature field at position x and time t.
t	time.
t_σ	scale time.
u	Darcy fluid velocity.
$\overline{V}_m$	molar volume of the mth mineral.
v	average fluid velocity.
v_l	velocity of the lth reaction front.
v_m; $v_m^{(i)}$	reaction front velocity of the mth mineral (at the ith zone boundary).
$W(k, D, u)$	factor in the expression for the equilibration length q for combined advection-diffusion.
x	spatial coordinate.
x_σ	scaled spatial coordinate.
γ_j, γ_i	aqueous activity coefficients for the jth primary species and ith complex.
$\eta(x, t)$	similarity variable for pure diffusive transport.
$\eta_m^{(i)}$	similarity variable for pure diffusive transport for the mth mineral at the ith zone boundary.
$\vartheta(x)$	Heaviside function.
λ	characteristic diffusion length.
ν_{ji}^{aq}	stoichiometric reaction matrix for reversibly reacting aqueous complexes.
ν_{jm}	stoichiometric reaction matrix for mineral reactions.
ξ_m	coefficient varying between zero and one.
σ	scaling parameter.
τ_0	time for mineral to dissolve completely at inlet.
ϕ	porosity.
ϕ_m	volume fraction of the mth mineral.
ϕ_m^∞	initial volume fraction of the mth mineral.
$\phi_s(x, t)$	solid phase volume fraction in the single component system.
ϕ_s^∞	initial solid phase volume fraction in the single component system.
$\chi(l; k)$	quantity in the reaction front velocity in the single component system.
Ψ_j	generalized concentration of the jth primary species in a multicomponent system.
Ψ_j^0	generalized inlet concentration of the jth primary species.
Ω_j	generalized flux of the jth primary species in a multicomponent system.
Ω_j^σ	scaled generalized flux.
$\tilde{(\ )}$	designation for a local equilibrium quantity.

INTRODUCTION

A quantitative time-space description of transport of solute species and their chemical interaction with minerals has the potential of providing a powerful new tool for analyzing many diverse geochemical processes. With the help of the quasi-stationary state approximation it is now possible to carry out numerical calculations of complex geochemical systems evolving over geologic time spans (Lichtner, 1988; Balashov and Lebedeva, 1991; Lichtner, 1991; Lichtner and Biino, 1992; Lichtner and Waber, 1992). However a quantitative description of natural systems often involves many uncertainties associated with initial and boundary conditions, heterogeneities in the flow system, and uncertainties in describing mineral reaction rates. The reaction mechanism of mineral reactions may range from surface to transport controlled depending on the magnitude of the rate constant and the rate of solute transport. As a consequence the reaction rate may be influenced by the geometry of the system resulting from the existence of boundary layers surrounding mineral grains in systems involving a flowing fluid (Murphy, Oelkers, and Lichtner, 1989). Uncertainties arise in incorporating nucleation kinetics and in the lack of a complete understanding of the reaction mechanism and form of the rate law (Steefel and Van Cappellen, 1990). Kinetic rate laws and their associated rate constants are known for only very few minerals for both dissolution and precipitation. An added difficulty in describing mineral reactions is quantifying mineral surface areas and its change with reaction. For example, the surface area of a dissolving mineral may either increase with reaction progress as a result of etch pit formation or decrease as mineral grains dissolve completely. Since the reaction rate is proportional to the surface area, the uncertainty in surface area can lead to substantial uncertainty in predicting the rate of reaction.

This contribution demonstrates that the effects of these uncertainties on solutions to kinetic mass transport equations may not be as significant as previously thought, especially for geochemical processes involving sufficiently long time spans. This is a consequence of the scaling properties of solutions to the kinetic mass transport equations. Scaling the kinetic rate constants by a common factor, which preserves their ratios, is equivalent to scaling the time and space coordinates of the original solution and the diffusion coefficient by the reciprocal factor. This result has far reaching consequences on the possible form of solutions to the kinetic transport equations. Because scaling the time and space coordinates merely stretches or shrinks the spatial profile of the solute concentration or mineral volume fraction without altering its magnitude, the reaction zone sequence and relative maxima and minima are preserved. As the scale factor approaches infinity, it follows that a kinetic solution to the transport equations must yield the same relative maxima and minima for the concentrations of solute species and mineral volume fractions as the corresponding local equilibrium solution. It further follows from the scaling relations that the velocities of propagation of the boundaries of

mineral alteration zones, or reaction fronts, become equal to their local equilibrium counterparts with increasing time under very general circumstances. This result was obtained previously by different methods (Ortoleva and others, 1986; Lichtner, 1988, 1991). Finally, solutions to kinetic transport equations belonging to different *relative* rate constants must scale to the identical local equilibrium solution provided it is unique.

The scaling properties of the kinetic transport equations do not depend on specific models used to describe, for example, the change in surface area or permeability with mineral reaction, provided these relations are scale independent. In this sense the scaling properties are model independent. This observation has important consequences for quantitatively describing mass transport processes in natural systems characterized by large inherent uncertainties.

SCALING PROPERTIES OF KINETIC MASS TRANSPORT EQUATIONS

Scaling relations may place severe restrictions on the time-space behavior of quantities defined through solutions to a system of partial differential equations. Although investigating the properties of solutions to differential equations by scaling the independent variables is a well know technique, it does not appear to have been applied previously to mass transport problems involving mineral precipitation-dissolution reactions. These equations are complicated by the presence of moving boundaries delineating different reaction zones.

Scale Transformation

An example of a scale transformation applied to a function of a single variable is illustrated in figure 1. Scaling the x-coordinate by the constant factor σ leads to the scaled function f_σ defined by

$$f_\sigma(x) = f(\sigma^{-1}x), \tag{1}$$

and therefore the point $\sigma^{-1}\,x$ is transformed to the point x preserving the value of the function f. As is apparent from the figure, the function is stretched or shrunk depending on the size of σ. Shrinking takes place if $\sigma < 1$, and stretching if $\sigma > 1$. Characteristic features of the function f(x) such as discontinuities, relative minima, maxima, and inflection points are all preserved in the scaled function f_σ. Thus, for example, at a relative maximum or minimum x_0, the first derivative of the function f(x) vanishes according to the equation

$$\frac{df}{dx}(x_0) = 0. \tag{2}$$

For the scaled function f_σ it follows that

$$\frac{df_\sigma}{dx}(\sigma x_0) = \sigma^{-1}\frac{df}{dx}(x_0) = 0, \tag{3}$$

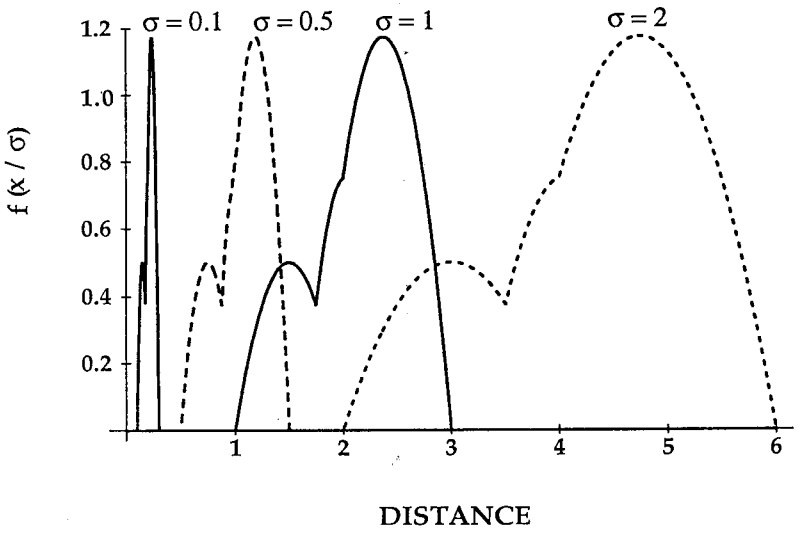

Fig. 1. Scaling transformation applied to a function f(x) of a single variable. Profiles are shown for f(σx) with σ = 0.1, 0.5, 1, and 2.

and therefore the scale transformation preserves the property of a relative maximum or minimum. A similar relation holds for inflection points defined by vanishing of the second derivative.

The scale transformation of the time and space coordinates of the form

$$x_\sigma = \sigma^{-1}x, \tag{4}$$

$$t_\sigma = \sigma^{-1}t, \tag{5}$$

with constant scale factor σ, applied to some function f(x, t) results in the transformed function $f_\sigma(x, t)$ defined by

$$f_\sigma(x, t) = f(x_\sigma, t_\sigma). \tag{6}$$

The inverse transformation is defined by

$$f(x, t) = f_\sigma(\sigma x, \sigma t). \tag{7}$$

The function f may correspond, for example, to field variables such as solute concentrations, mineral volume fractions, temperature, and pressure. As an example, consider the function φ(x, t) defined by the equation

$$\phi(x, t) = \begin{cases} \dfrac{\phi_0}{(v_2 - v_1)t}(v_2 t - x) & (v_1 t \le x \le v_2 t) \\ 0 & \text{otherwise} \end{cases}, \tag{8}$$

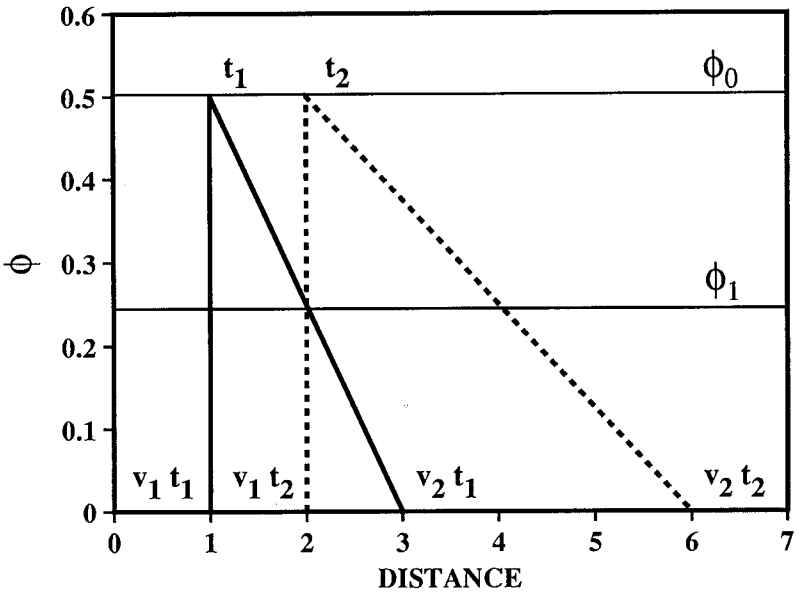

Fig. 2. Illustration of a traveling wave. The traveling wave is invariant under a scale transformation of both the space and time coordinates.

where ϕ_0, v_1, and v_2 are constants. The function $\phi(x, t)$ represents a traveling wave as illustrated in figure 2 for two different times, t_1 and t_2. As defined, clearly ϕ satisfies the scaling relation

$$\phi(\sigma x, \sigma t) = \phi(x, t), \tag{9}$$

and thus is invariant under a scale transformation. Another interesting feature of the function ϕ is the transformation property of the function giving the position of a constant value of ϕ with time. This function, denoted by $l(t)$, is defined implicitly by the relation

$$\phi(l(t), t) = \phi_1 = \text{constant}. \tag{10}$$

It follows that $l(t)$ is given explicitly by the expression

$$l(t) = \left[\left(1 - \frac{\phi_1}{\phi_0}\right) v_2 + \frac{\phi_1}{\phi_0} v_1\right] t. \tag{11}$$

The velocity at which this point moves is given by

$$v_l = \frac{dl}{dt} = \left[\left(1 - \frac{\phi_1}{\phi_0}\right) v_2 + \frac{\phi_1}{\phi_0} v_1\right]. \tag{12}$$

From these relations the scaling properties of $l(t)$ and v_l follow given by the expressions:

$$l(\sigma t) = \sigma l(t), \tag{13}$$

and

$$v_l(\sigma t) = v_l(t) = \text{constant}. \tag{14}$$

This simple example is useful for investigating the scaling properties of chemical reaction fronts as demonstrated below.

Application of the scaling relations to the non-reactive mass transport equation is presented in app. A. In what follows it is assumed that the reader is familiar with the general form of the reactive mass transport equations. Before proceeding to the general case of the transport equations in an open system, first the simpler case of a closed system is considered.

Closed System

The mass transfer equations for a well-mixed, closed system may be expressed in the form

$$\frac{d\Psi_j}{dt} = -\sum_m \nu_{jm} I_m, \tag{15}$$

and

$$\frac{dn_m}{dt} = I_m, \tag{16}$$

for aqueous species and minerals, respectively. In these equations n_m and I_m denote the number of moles and reaction rate, respectively, of the mth mineral, Ψ_j denotes the generalized concentration of the jth primary species with concentration C_j, defined by

$$\Psi_j = C_j + \sum_i \nu_{ji}^{aq} C_i, \tag{17}$$

where the subscript i refers to aqueous complexes with concentration C_i, and ν_{ji}^{aq} refers to the corresponding stoichiometric reaction coefficients. It is assumed that local equilibrium holds within the aqueous phase with the concentrations of aqueous complexes related to concentrations of the primary species by mass action equations. The quantity ν_{jm} denotes the stoichiometric coefficient for reaction of the mth mineral with the aqueous solution. These equations are subject to the initial conditions

$$\Psi_j(0) = \Psi_j^0, \tag{18}$$

and

$$n_m(0) = n_m^0. \tag{19}$$

In a kinetic representation of mineral reactions the reaction rate I_m is specified as some known function of the concentrations of the primary species, which are used to characterize the system. The basic requirement that must be satisfied by the rate law is that the reaction rate tend toward zero as equilibrium is approached. One form for the kinetic rate of mineral reactions consistent with transition state theory (Aagaard and Helgeson, 1982) is given by

$$I_m = -k_m s_m\{1 - \exp[-\mathbf{A}_m/RT]\}, \tag{20}$$

where k_m denotes the kinetic rate constant, s_m denotes the reacting surface area, $\mathbf{A}_m$ denotes the chemical affinity, and R and T denote the gas constant and temperature, respectively. The quantity in curly brackets containing the affinity in the rate expression ensures that the reaction rate vanishes at equilibrium. The rate is taken as positive for precipitation and negative for dissolution, with units of moles per unit volume per unit time. An essential feature of the rate law regarding the scaling properties of the solution is its linear dependence on the kinetic rate constant.

Scaling the time coordinate according to eq (5) leads to the transformed equations

$$\frac{d\Psi_j}{dt_\sigma} = -\sigma \sum_m \nu_{jm} I_m; \tag{21}$$

and

$$\frac{dn_m}{dt_\sigma} = \sigma I_m. \tag{22}$$

Noting that the kinetic rate I_m is proportional to the kinetic rate constants k_m, the scaled equations are identical in form to eqs (15) and (16) if k_m is replaced by σk_m for all reacting minerals. Consequently, because the initial and boundary conditions are invariant under the scale transformation, these equations must have solutions identical to the original equations, and therefore it follows that $\Psi_j(t; \{k\})$ scales with time according to the relation

$$\Psi_j(\sigma^{-1}t; \sigma\{k\}) = \Psi_j(t; \{k\}), \tag{23}$$

with $\sigma\{k\} = \{\sigma k_1, \ldots, \sigma k_M\}$ or, alternatively

$$\Psi_j(t; \sigma\{k\}) = \Psi_j(\sigma t; \{k\}). \tag{24}$$

A similar result holds for the function $n_m(t)$. Therefore if a solution is known for one set of kinetic rate constants, it can be obtained for any other set that preserves their ratios, merely by scaling the time t. Thus the reaction path followed by the system is identical for both sets of rate constants; however, the velocity of the system point as it moves along the path is greater the larger the rate constants. The sequence of secondary

minerals formed, therefore, is also the same, only the times at which they occur along the reaction path are different related by the scale factor.

Changing the relative values of the rate constants leads, in general, to a different reaction path and may involve formation of different secondary minerals. However, because the system is closed, the final equilibrium state of the system is a function only of its initial state and must be independent of the particular reaction path taken by the system and hence the kinetic rate constants.

Open System

In an open system involving advective and diffusive mass transport, the equations describing the system are given by

$$\frac{\partial}{\partial t}(\phi\Psi_j) + \frac{\partial \Omega_j}{\partial x} = -\sum_m \nu_{jm} I_m, \tag{25}$$

for solute species, where Ω_j denotes the generalized flux consisting of contributions from advection and diffusion defined by

$$\Omega_j = -\phi D \frac{\partial \Psi_j}{\partial x} + u\Psi_j, \tag{26}$$

where D denotes the diffusion coefficient considered to be the same for all species, for simplicity, and u designates the Darcy velocity, in general a function of time and distance, and

$$\frac{\partial \phi_m}{\partial t} = \overline{V}_m I_m, \tag{27}$$

for minerals (for more details, see Lichtner, 1985, 1992). These equations are based on a continuum representation of a porous medium. Definitions of the variables used in these equations can be found in the list of symbols.

The transport equations are subject to initial conditions specifying the modal composition of the unreacted rock, the composition of the fluid occupying the pore spaces at t = 0, and boundary conditions specifying the composition of the fluid entering the porous medium at the inlet. The initial fluid composition is specified by the quantity Ψ_j^∞ according to the equation

$$\Psi_j(x, 0) = \Psi_j^\infty, \tag{28}$$

and the initial modal composition of the host rock by ϕ_m^0 according to

$$\phi_m(x, 0) = \phi_m^0. \tag{29}$$

The composition of the fluid at the inlet specified by Ψ_j^0 is defined through the boundary condition

$$\Psi_j(0, t) = \Psi_j^0. \tag{30}$$

Other boundary conditions are also possible, for example, by specifying the fluid flux at the inlet. For the scaling relations to be applicable it is necessary that the initial and boundary conditions remain invariant under a scale transformation, which rules out the flux boundary condition.

Although the positions of the boundaries of the various reaction zones provide convenient quantities with which to describe the system, they do not appear explicitly in the kinetic transport equations. They are, however, implicitly contained in the functions representing the mineral volume fractions. This is in contrast to a local equilibrium description in which the positions of the various reaction fronts are essential variables for describing the system as it evolves in time. In a kinetic description it is possible to define the position of the ith reaction zone boundary corresponding to the mth mineral, denoted by l_m, by the equation

$$\phi_m(l_m(t), t) = \text{constant}. \tag{31}$$

Note that this equation applies to the end points of a reaction zone by taking the constant equal to zero, where the modal abundances vanish as a consequence of the finite rates of reaction. Often, however, a reaction zone is further divided into subzones. At the boundaries of these subzones the modal abundances need not vanish. In a local equilibrium description jump discontinuities occur across the boundaries of the subzones as well as the end points of the zone. However, for each reaction front it is always possible to find at least one mineral for which its modal abundance vanishes. For a non-zero value of the constant, this definition of the position of a reaction front includes fronts contained within a reaction zone, determined by a constant value of the modal composition of some mineral. This definition of a reaction front only holds asymptotically after the system achieves a steady-state, and the front velocities become constant. For diffusive transport under conditions of local equilibrium the mineral modal abundances are rigorously constant at each front for all time starting at $t = 0$ (Lichtner and Balashov, 1992). However, for combined advection and diffusion, in general the mineral modal compositions at the various reaction fronts change with time approaching a constant value asymptotically.

The reaction front velocities are obtained by differentiating the above equation with respect to time to give

$$v_m = -\frac{\partial \phi_m / \partial t}{\partial \phi_m / \partial x}. \tag{32}$$

The front velocities are useful quantities for comparing the rate of weathering of different minerals, for example.

As in a closed system, because the reaction rate I_m of the mth mineral, defined in eq (20), is proportional to the kinetic rate constant k_m, the transport equations are linear in the rate constants. This circumstance leads to significant implications on the possible form of solutions to

the kinetic mass transport equations for rate constants that differ by a constant scale factor. Scaling properties of the kinetic mass transport equations follow directly from eqs (25) and (27). These properties are more complicated than the non-reactive transport equations due to the presence of reaction fronts. Scaling the time and space coordinates by the factor σ according to eqs (4) and (5) leads to the transformed transport equations

$$\frac{\partial}{\partial t_\sigma}(\phi\Psi_j) + \frac{\partial \Omega_j^\sigma}{\partial x_\sigma} = -\sigma \sum_m \nu_{jm} I_m, \tag{33}$$

and

$$\frac{\partial \phi_m}{\partial t_\sigma} = \sigma \bar{V}_m I_m, \tag{34}$$

where the transformed generalized flux Ω_j^σ is defined by

$$\Omega_j^\sigma = -\phi\sigma^{-1} D \frac{\partial \Psi_j}{\partial x_\sigma} + u\Psi_j. \tag{35}$$

Both eqs (33) and (34) have the identical form as the original transport equations given by eqs (25) and (27), if $\{k\}$ is replaced by $\sigma\{k\}$, and D is replaced by σ^{-1} D. Furthermore, both sets of equations are subject to the identical initial and boundary conditions given by eqs (28), (29), and (30) which are invariant under the scale transformation. Therefore a solution to the scaled transport equations is related to the corresponding solution to the original equations according to

$$\Psi_j(x_\sigma, t_\sigma; \sigma\{k\}, \sigma^{-1}D, u) = \Psi_j(x, t; \{k\}, D, u), \tag{36}$$

and

$$\phi_m(x_\sigma, t_\sigma; \sigma\{k\}, \sigma^{-1}D, u) = \phi_m(x, t; \{k\}, D, u), \tag{37}$$

where the functions on the left hand side of these relations are solutions to eqs (33) and (34), and the functions on the right hand side to eqs (25) and (27).

Just as it is possible to deduce the behavior of the solution to the non-reactive transport equation on the diffusion coefficient directly from the scaling relation (see app. A), in this case it is possible, in addition, to investigate the behavior of the solution on the kinetic rate constants. To this end it is convenient to introduce the field variable $F_\alpha(x, t; \{k\}, D, u)$ and rewrite eqs (36) and (37) in the general form

$$F_\alpha(x_\sigma, t_\sigma; \sigma\{k\}, \sigma^{-1}D, u) = F_\alpha(x, t; \{k\}, D, u), \tag{38}$$

where F_α signifies the quantities Ψ_j and ϕ_m. This relation may be expressed in the equivalent form

$$F_\alpha(x, t; \sigma\{k\}, \sigma^{-1}D, u) = F_\alpha(\sigma x, \sigma t; \{k\}, D, u), \tag{39}$$

in which x is replaced by σx and t by σt. Thus scaling the rate constants by a common factor and the diffusion coefficient by the reciprocal factor is equivalent to scaling the time and space coordinates by the same factor. From this equation the behavior of the system for different kinetic rate constants and different diffusion coefficients related by the scale factor σ to the original constants can be deduced. It must be emphasized that in order for the scaling relation to hold, all rate constants must be scaled by the same factor σ. Changing the relative kinetic rate constants in general leads to an entirely different solution with a different sequence of reaction zones. However, as discussed below, for sufficiently long time spans all solutions must tend to the same asymptotically limiting solution, provided it is unique, regardless of the choice of rate constants.

An immediate consequence of eq (39) for a system undergoing pure advective transport is the scaling relation

$$F_\alpha(x, t; \sigma\{k\}, u) = F_\alpha(\sigma x, \sigma t;\{k\}, u). \tag{40}$$

Thus scaling the time and space coordinates by a common factor is equivalent to scaling the kinetic rate constants by the same factor. Note that no assumptions are made regarding the particular models that may be used to represent mineral surface area, porosity, or permeability. They may be described by any scale invariant function of the mineral volume fractions, for example. Hence in this sense the scaling relations are model independent.

Zone boundary positions and reaction front velocities.—From the scaling relation satisfied by the mineral volume fraction, it is possible to derive scaling properties for the positions of the reaction zone boundaries or reaction fronts and their velocities. The position of the ith reaction front corresponding to the mth mineral, $l_m^{(i)}(t; \{k\}, D, u)$, is defined implicitly by the relation

$$\phi_m(l_m^{(i)}(t; \{k\}, D, u), t; \{k\}, D, u) = \text{constant}, \tag{41}$$

according to eq (31). Likewise the position of the reaction front, $l_m^{(i)}(t; \sigma\{k\}, \sigma^{-1}D, u)$, corresponding to the scaled transport equations satisfies a similar equation

$$\phi_m(l_m^{(i)}(t; \sigma\{k\}, \sigma^{-1}D, u), t; \sigma\{k\}, \sigma^{-1} D, u) = \text{constant}. \tag{42}$$

Making use of the scaling properties of ϕ_m, the latter relation can be expressed as

$$\phi_m(\sigma l_m^{(i)}(t; \sigma\{k\}, \sigma^{-1}D, u), \sigma t; \{k\}, D, u) = \text{constant}. \tag{43}$$

Note that in this expression l_m is evaluated at time t and not σt. Comparing this equation with eq (41) in which t is replaced by σt leads to the scaling relation for the reaction zone boundaries:

$$\sigma l_m^{(i)}(t; \sigma\{k\},\sigma^{-1}D, u) = l_m^{(i)}(\sigma t; \{k\}, D, u). \tag{44}$$

This relation is analogous to the transformation of the spatial coordinate x. Thus the position of the reaction front at time σt, corresponding to rate constants $\{k\}$ and diffusion coefficient D, is equal to σ times the position of the front at time t corresponding to the scaled rate constants $\sigma\{k\}$ and diffusion coefficient σ^{-1} D.

The scaling relation for the reaction front velocities follows from the definition

$$v_m^{(i)}(t; \{k\}, D, u) = \frac{d}{dt} l_m^{(i)}(t; \{k\}, D, u). \tag{45}$$

Differentiating both sides of eq (44) with respect to time yields the scaling relation

$$v_m^{(i)}(t; \sigma\{k\}, \sigma^{-1}D, u) = v_m^{(i)}(\sigma t; \{k\}, D, u), \tag{46}$$

in which the scaling factor σ cancels. According to this result by scaling the time coordinate the velocities of the zone boundaries are related to the velocities corresponding to the solution with scaled rate constants $\sigma\{k\}$ and diffusion coefficient σ^{-1} D at time t.

Local Equilibrium Limit

A solution to the kinetic transport equations approaches the local equilibrium limiting solution as the rate constants grow without bound according to the relation:

$$\lim_{\{k\}\to\infty} F_\alpha(x, t; \{k\}, D, u) \to \tilde{F}_\alpha(x, t; D, u), \tag{47}$$

where $\tilde{F}_\alpha(x, t; D, u)$ designates field variables corresponding to conditions of local equilibrium as defined in app. B. By simultaneously considering the limit in which $\{k\} \to \infty$ and $D \to 0$, the pure advective local equilibrium limit is obtained:

$$\lim_{\substack{\{k\}\to\infty \\ D\to 0}} F_\alpha(x, t; \{k\}, D, u) \to \tilde{F}_a(x, t; u). \tag{48}$$

These relations may be taken as the definition of the local equilibrium limit.

To investigate the implications of the scaling properties on the relation between the kinetic solution and the local equilibrium limiting solution, consider the limit $\sigma \to \infty$ applied to eq (39). The right hand side of this equation tends, by definition, to the local equilibrium limit corresponding to pure advective transport as follows from eq (48). Therefore by scaling the time and space coordinates of the kinetic solution $F_\alpha(x, t; \{k\}, D, u)$ corresponding to fixed rate constants $\{k\}$, the kinetic solution can be made to approach arbitrarily close to the pure advective local equilibrium limiting solution according to

$$\lim_{\sigma\to\infty} F_\alpha(\sigma x, \sigma t; \{k\}, D, u) = \lim_{\sigma\to\infty} F_\alpha(x, t; \sigma\{k\}, \sigma^{-1}D, u) \to \tilde{F}_i(x, t; u). \tag{49}$$

The reaction zone boundaries and velocities also approach their limiting values corresponding to the pure advective local equilibrium limit:

$$\lim_{\sigma\to\infty} \frac{1}{\sigma} l_m^{(i)}(\sigma t; \{k\}, D, u) = \lim_{\sigma\to\infty} l_m^{(i)}(t; \sigma\{k\}, \sigma^{-1}D, u) \to \tilde{l}_m^{(i)}(t; u), \qquad (50)$$

and

$$\lim_{\sigma\to\infty} v_m^{(i)}(\sigma t; \{k\}, D, u) = \lim_{\sigma\to\infty} v_m^{(i)}(t; \sigma\{k\}, \sigma^{-1} D, u) \to \tilde{v}_m^{(i)}. \qquad (51)$$

These relations are of fundamental importance. They imply that after a sufficient amount of time has elapsed the profiles of the solute concentration and mineral volume fraction obtained from the kinetic transport equations bear a strong resemblance to the corresponding local equilibrium solution. Merely by scaling both the time and space coordinates of the kinetic solution, it is possible to extract the local equilibrium limiting solution for any arbitrary set of rate constants. A scale transformation of the spatial coordinate does not change the amplitude of the solute concentration or mineral volume fraction but only stretches or shrinks the spatial profile. Therefore given a sufficiently long time span, a kinetic solution belonging to finite rate constants preserves maxima and minima of the corresponding local equilibrium solution. The widths of the various reaction zones and the shapes of the concentration and volume fraction profiles, however, are different in the kinetic solution.

In an isothermal system the solution to the kinetic transport equations approaches asymptotically a steady-state in which the various reaction zones propagate with constant velocity. The local equilibrium velocities $\tilde{v}_m^{(i)}$ corresponding to pure advective transport in an isothermal system are also independent of time as are the solute concentrations and mineral modal abundances within each reaction zone. Therefore it follows from eq (51) that if $\tilde{v}_m^{(i)}$ obtained from a kinetic solution is also constant independent of the time, it must be identical to the local equilibrium limiting value $\tilde{v}_m^{(i)}$. Thus the reaction front velocities in a kinetic description approach asymptotically the local equilibrium limiting values. This result has been obtained previously using different methods by Ortoleva and others (1986) and Lichtner (1988).

The asymptotic solution to the kinetic transport equations may be depicted as a traveling wave which does not change shape in the vicinity of each reaction front. The velocity of the ith reaction front $l_i(t)$ in the traveling wave approximation is given by Lichtner (1988)

$$v_i = \frac{dl_i}{dt} = \frac{\langle \Omega_j \rangle_i}{\langle \phi \Psi_j \rangle_i + \sum \nu_{jm} \bar{V}_m^{-1} \langle \phi_m \rangle_i}. \qquad (52)$$

In this equation the angular brackets $\langle \ldots \rangle_i$ denote the difference in the enclosed quantity across the ith reaction front. If the solute concentration comes to equilibrium with the minerals on either side of the front, this

expression reduces to the Rankine-Hugoniot equations, and the velocities of the fronts are identical to that obtained from local equilibrium considerations. Normally reaction zones increase in width at a constant velocity. Special zones, referred to as ghost zones, have a constant width and are governed by diffusive transport (Lichtner and Balashov, 1992). In a local equilibrium description their width approaches zero in the limit as the diffusion coefficient tends to zero.

Sensitivity of the solution to kinetic rate constants.—As demonstrated above, a solution to the kinetic transport equations for a finite set of rate constants {k} can be made to approach as closely as desired to the local equilibrium limiting solution corresponding to pure advective transport by scaling the time and space coordinates. Since this statement is true regardless of the choice of rate constants {k}, it further follows that two solutions with the same initial and boundary conditions but corresponding to different sets of kinetic rate constants must scale to the same local equilibrium limiting solution. This is true provided the local equilibrium solution is unique. In addition the sequence of reaction zones in the steady-state limit must be the same as determined from the corresponding local equilibrium solution. Thus altering the kinetic rate constants cannot affect the reaction zone sequence. From these results it can be concluded that for sufficiently large time spans kinetics plays a minor role in determining the behavior of the system.

It should be kept in mind, however, that a solution corresponding to finite rate constants {k} does *not* strictly approach the local equilibrium solution with increasing time. Rather only the kinetic solution scaled in both the time and space coordinate approaches arbitrarily close to the local equilibrium solution as the scale factor tends to infinity. However, the interior region of a reaction zone approaches the local equilibrium limit more rapidly than the region in the neighborhood of a reaction front.

Pure Diffusion

So far the discussion has focused on transport involving both advection and diffusion. Similar results can be derived for pure diffusive transport. In this case it is useful to consider a slightly different scale transformation of the form (Balashov and Lebedeva, 1991)

$$x_\sigma = x/\sqrt{\sigma}, \tag{53}$$

and

$$t_\sigma = t/\sigma. \tag{54}$$

As pointed out by Balashov (private communication), this relation may be derived by considering the more general transformation:

$$x' = ax, \tag{55}$$

and

$$t' = bt, \tag{56}$$

where a and b are arbitrary real numbers. Solutions to the combined advection and diffusion kinetic transport equations then scale according to

$$F(ax, bt; \{k\}, D, u) = F(x, t; b^{-1}\{k\}, a^2b^{-1}D, ab^{-1}u). \tag{57}$$

The previous transformation defined by eqs (4) and (5) is obtained by demanding that the coefficient multiplying u be unity, or

$$\sigma^{-1} = a = b. \tag{58}$$

The transformation for pure diffusive transport given by eqs (53) and (54) follows from the condition

$$b = a^2, \tag{59}$$

giving unit coefficient multiplying D. With this transformation solutions to the pure diffusion kinetic transport equations scale according to

$$F_\alpha(\sqrt{\sigma}x, \sigma t; \{k\}, D) = F_\alpha(x, t; \sigma\{k\}, D), \tag{60}$$

in which the diffusion coefficient remains unchanged. The reaction zone boundaries and reaction front velocities satisfy the relations

$$\frac{1}{\sqrt{\sigma}} l_m^{(i)}(\sigma t; \{k\}, D) = l_m^{(i)}(t; \sigma\{k\}, D), \tag{61}$$

and

$$\sqrt{\sigma} v_m^{(i)}(\sigma t; \{k\}, D) = v_m^{(i)}(t; \sigma\{k\}, D). \tag{62}$$

Under the scale transformation given by eqs (53) and (54), the local equilibrium limiting solution has the property that it is invariant:

$$\tilde{F}_\alpha(\sqrt{\sigma}x, \sigma t; D) = \tilde{F}_\alpha(x, t; D). \tag{63}$$

This result implies that the pure diffusion moving boundary problem can be described in terms of a single variable η, referred to as the Stefan variable, defined by

$$\eta(x, t) = \frac{x}{2\sqrt{Dt}}. \tag{64}$$

This result has been used by Novak, Schechter, and Lake (1989) to obtain solutions for pure diffusion. The positions of reaction fronts are given by

$$\tilde{l}_m^{(i)} = 2\eta_m^{(i)}\sqrt{Dt}, \tag{65}$$

with the corresponding velocities

$$\tilde{v}_m^{(i)} = \eta_m^{(i)} \sqrt{\frac{D}{t}}, \tag{66}$$

for constants $\eta_m^{(i)}$. These quantities are not invariant but scale according to the relations

$$\frac{1}{\sqrt{\sigma}} \tilde{l}_m^{(i)}(\sigma t; D) = \tilde{l}_m^{(i)}(t; D), \tag{67}$$

and

$$\sqrt{\sigma} \tilde{v}_m^{(i)}(\sigma t; D) = \tilde{v}_m^{(i)}(t; D), \tag{68}$$

similar to the kinetic case.

From the scaling relations it follows that the limit of the kinetic solution as $\sigma \to \infty$ approaches the corresponding local equilibrium solution according to

$$\lim_{\sigma\to\infty} F_\alpha(\sqrt{\sigma}x, \sigma t; \{k\}, D) = \lim_{\sigma\to\infty} F_\alpha(x, t; \sigma\{k\}, D) \to \tilde{F}_\alpha(x, t; D). \tag{69}$$

Likewise the reaction front positions and velocities approach the corresponding local equilibrium limit. For example it follows that

$$\lim_{\sigma\to\infty} \frac{l_m^{(i)}(\sigma t; \{k\}, D)}{\tilde{l}_m^{(i)}(\sigma t; D)} = \lim_{\sigma\to\infty} \frac{l_m^{(i)}(t; \sigma\{k\}, D)}{\tilde{l}_m^{(i)}(t; D)} = 1, \tag{70}$$

with a similar result for the reaction front velocities.

EXAMPLES

In this section several examples are presented illustrating the scaling properties of the kinetic mass transport equations. The relation between solutions based on a kinetic description of mineral reaction rates and the corresponding local equilibrium limit are investigated.

Single Component System

The first example considers a single component system. As a fluid undersaturated with respect to a solid phase infiltrates or diffuses into a porous column containing the solid, the solid dissolves producing a reaction front l(t) that advances with time in the direction of flow. The problem is to determine the position of the dissolution front as a function of time and the concentration profile of the solute species and modal composition of the solid as functions of time and distance.

For the simple system involving the reaction of a single component mineral such as quartz according to a linear rate law, an analytic solution to the transport equations exists based on the quasi-stationary state

approximation assuming constant porosity, permeability, and mineral surface area (Lichtner, 1988). In this approximation the partial time derivative contained in the transient solute transport equations is neglected. The transport equations take the form

$$\phi D \frac{d^2C}{dx^2} - u \frac{dC}{dx} = ks(C - C_{eq})\theta(x - l(t)), \tag{71}$$

for the solute species, and

$$\frac{\partial \phi_s}{\partial t} = ks\overline{V}_s(C - C_{eq})\theta(x - l(t)), \tag{72}$$

for the solid phase, where C denotes the solute concentration, k denotes the kinetic rate constant, s denotes the specific surface area, C_{eq} denotes the equilibrium concentration, and ϕ_s and $\overline{V}_s$ denote the volume fraction and molar volume of the solid phase, respectively. The function $\theta(x)$ denotes the Heaviside function equal to one if $x \geq 0$, and zero otherwise. The position of the dissolution front is denoted by l(t). These equations are solved subject to the initial and boundary conditons

$$C(0, t) = C_0, \tag{73}$$

and

$$\phi_s(x, 0) = \phi_s^\infty, \tag{74}$$

determining the inlet fluid composition and initial solid modal composition, respectively. The moving boundary problem posed by these equations requires determining the solute concentration C(x, t; k, D, u), mineral volume fraction ϕ_s(x, t; k, D, u), and position of the dissolution front l(t; k, D, u). The solution to these equations is given in app. C.

The scaling properties of the quartz dissolution front determined from eq (C.26) is illustrated in figure 3 where the reaction front position is plotted as a function of time for σ = 1, 2, and 10. Also shown in the figure is the local equilibrium limit for pure advection (dashed-dotted line) and combined advection and diffusion. For this example $k = 10^{-10}$ moles $cm^{-2}\,s^{-1}$, $s = 1\ cm^{-1}$, $D = 5 \times 10^{-4}\ cm^2\,s^{-1}$, $u = 1\ m\,y^{-1}$, $C_{eq} = 10^{-3}$ moles $liter^{-1}$, $\phi_s^\infty = 0.9$, and $C_0 = 0$. The values for k, s, and C_{eq} correspond approximately to the dissolution of quartz at 100°C for a grain size of 1 mm. As time increases the front velocities become constant approaching the pure advective local equilibrium limit, with the positions of the fronts displaced by the characteristic diffusion length $\lambda = \phi D/u \simeq 15$ cm. As σ increases, the position of the front described by the kinetic formulation approaches the pure advective local equilibrium result. The thin dashed lines illustrate the scaling relation

$$l(2t; k, D) = 2l(t; 2k, D/2), \tag{75}$$

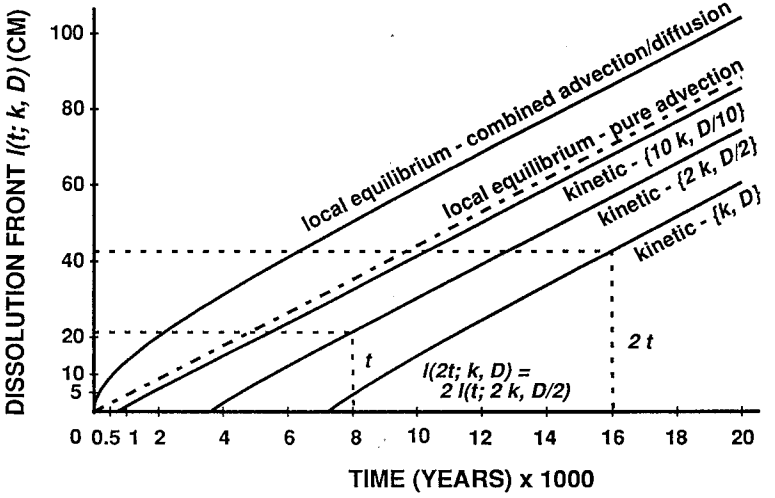

Fig. 3. Scaling properties of the dissolution front l(t; k, D, u) illustrated for a single component system. The position of the reaction front in centimeters is plotted as a function of time in years for kinetic and local equilibrium solutions to the transport equations. In addition the local equilibrium limit for combined advection and diffusion and pure advection (dashed-dotted line) are also shown.

showing the correspondence between the dissolution fronts with a scaling factor $\sigma = 2$ at times t = 8000 and 16,000 yrs.

Shown in figures 4 and 5 are the results of scaling the solute concentration and volume fraction defined by eqs (C.1) and (C.2), respectively. Both quantities are plotted as a function of distance for an elapsed time of 16,000 yrs with the origin of the coordinate system taken to coincide with the instantaneous position of the dissolution front. The solid line labeled $\sigma = \infty$ in figure 4 corresponds to the local equilibrium limit. At the reaction front the solute concentration is approximately constant as can be seen from the figure. The concentration decreases toward the inlet as a consequence of diffusive transport. As is apparent from the figures, with increasing σ the solution to the kinetic transport equations approaches the local equilibrium limit. It should be emphasized, however, that with increasing time for a fixed kinetic rate constant, the kinetic solution to the transport equations approaches a steady-state limit, given by the curves labeled $\sigma = 1$, which clearly does not correspond to the local equilibrium solution. Only by scaling both the time and space coordinates can the local equilibrium solution be extracted from the kinetic solution.

Application to Weathering

This section considers weathering of a hydrothermally altered phonolite host rock found in the Poços de Caldas alkaline complex. This

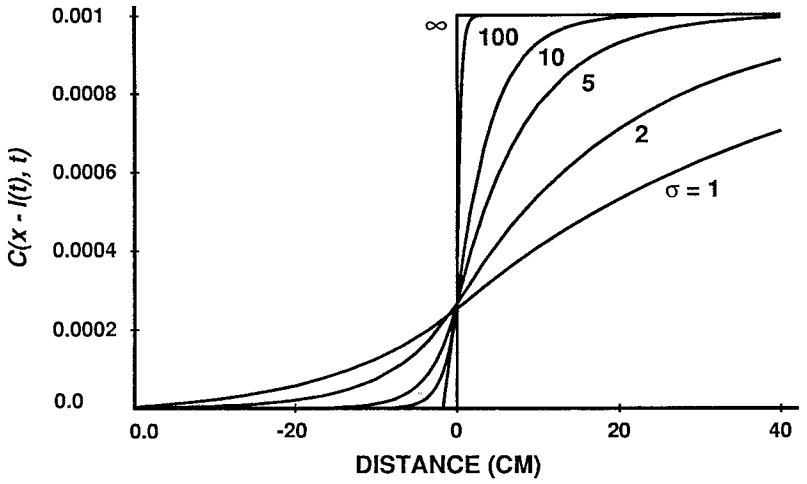

Fig. 4. Solute concentration C(x, t; σk, σ^{-1}D, u) plotted for t = 250 yrs as a function of distance relative to the instantaneous position of the dissolution front l(t; σk, σ^{-1}D, u) for scale factors σ = 1, 2, 5, 10, 100, and ∞. The local equilibrium solution corresponds to σ = ∞. The curves are calculated for the same conditions as in the previous figure. Note that the solute concentration at the reaction front becomes independent of the scaling factor as σ increases.

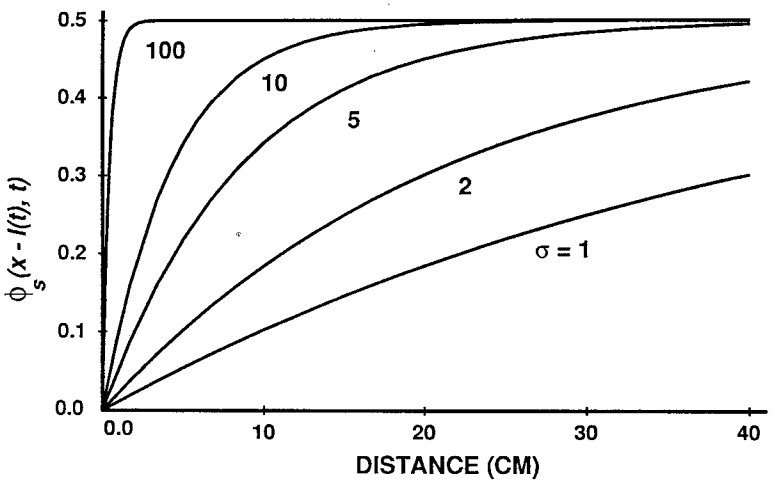

Fig. 5. Volume fraction plotted as a function of distance relative to the dissolution front for the same conditions as figure 3.

problem was considered previously as part of an international natural analogue project on the transport of uranium (Lichtner and Waber, 1992). There it was demonstrated that qualitative agreement with field observations conducted by Waber (ms) could be obtained by considering downward percolation of rainwater through a host rock consisting of the minerals K-feldspar, kaolinite, illite (as muscovite), and fluorite. In this work this example is used to illustrate the scaling properties of the kinetic transport equations.

This system is assumed to be described in terms of 9 primary species consisting of K^+, Na^+, Ca^{2+}, Al^{3+}, H^+, SiO_2, F^-, HCO_3^-, and Cl^-. Both Na^+ and Cl^- are inert but are included to describe the composition of the infiltrating rainwater. Thermodynamic data used in the calculation, with the exception of illite, were taken from the EQ3/6 database. The qualitative features of the resulting weathering profile are extremely sensitive to the value used for the illite log K. In this work a log K of -9.5 was chosen compared to the value of -11.02 for muscovite in the EQ3/6 database. The latter value was found to produce geologically unreasonable results resulting in the precipitation of large amounts of K-feldspar. The value used in the present work, however, does not result in as good a fit to field observations as the value of -10.4 used in Lichtner and Waber (1992). In that case, however, illite appears as a ghost zone requiring special considerations to obtain a proper solution (Lichtner and Balashov, 1992).

First the situation represented by local chemical equilibrium is considered. This results in a set of algebraic equations to determine the solute concentrations, mineral volume fractions, and reaction front velocities. The results of reaction of percolating rainwater through the hydrothermally altered phonolite host rock are presented in table 1. The details of the calculation may be found in Lichtner (1991). Here it is noted that the local equilibrium equations do not determine the sequence of reaction zones directly but only by trial and error methods involving iterating the zone sequence until a consistent solution is obtained. Five distinct alteration zones were found resulting in the zone sequence:

$$\mathrm{F|Gbs|Gbs - Kln|Ill|Kfs - Ill|Kfs - Ill - Fl|Kfs - Ill - Kln - Fl,}$$

where F denotes a zone consisting of fluid only with the composition of the infiltrating fluid. Note that kaolinite forms two distinct reaction zones: a zone at the top of the weathered column consisting of both primary and secondary kaolinite and primary kaolinite deeper in the profile.

Presented in table 1 are the pH, P_{CO_2}, concentrations for primary species, generalized concentrations Ψ_j and aqueous complexes, and mineral volume fractions for each reaction zone beginning with the inlet and ending with the unaltered host rock. The bottom two rows give the porosity ϕ and velocities of the various reaction fronts relative to the Darcy velocity v_0, respectively. The inlet fluid is taken as rainwater

TABLE 1

Results of a local equilibrium calculation with the identical inlet fluid composition and initial host rock composition as used in the corresponding kinetic calculation shown in figures 6 and 7. For sufficiently long elapsed time spans, the results show excellent agreement with the corresponding kinetic calculations

	inlet	zone 1	zone 2	zone 3	zone 4	zone 5	zone 6
pH	4.30	4.32	4.32	5.75	6.75	6.75	5.82
log P_{CO_2}	−2.00	−2.00	−2.00	−2.10	−2.55	−2.56	−2.11
				primary species			
K^+	1.00×10^{-5}	1.00×10^{-5}	1.00×10^{-5}	1.26×10^{-4}	3.06×10^{-4}	3.07×10^{-4}	1.11×10^{-4}
Na^+	2.74×10^{-5}	2.74×10^{-5}	2.74×10^{-5}	2.74×10^{-5}	2.74×10^{-5}	2.74×10^{-5}	2.74×10^{-5}
Ca^{2+}	5.00×10^{-6}	5.00×10^{-6}	5.00×10^{-6}	5.00×10^{-6}	4.99×10^{-6}	3.10×10^{-4}	3.18×10^{-4}
Al^{3+}	8.24×10^{-11}	7.55×10^{-7}	7.55×10^{-7}	3.93×10^{-11}	1.36×10^{-15}	1.60×10^{-15}	9.81×10^{-13}
$SiO_2(aq)$	1.00×10^{-6}	1.00×10^{-6}	5.68×10^{-5}	5.68×10^{-5}	5.95×10^{-4}	5.99×10^{-4}	1.72×10^{-3}
HCO_3^-	3.10×10^{-6}	3.25×10^{-6}	3.25×10^{-6}	7.07×10^{-5}	2.48×10^{-4}	2.48×10^{-4}	8.11×10^{-5}
F^-	1.00×10^{-10}	9.99×10^{-11}	9.99×10^{-11}	1.00×10^{-10}	1.00×10^{-10}	6.12×10^{-4}	6.00×10^{-4}
Cl^-	9.50×10^{-5}	9.50×10^{-5}	9.50×10^{-5}	9.50×10^{-5}	9.50×10^{-5}	9.50×10^{-5}	9.50×10^{-5}
				Ψ_j			
K^+	1.00×10^{-5}	1.00×10^{-5}	1.00×10^{-5}	1.26×10^{-4}	3.06×10^{-4}	3.07×10^{-4}	1.11×10^{-4}
Na^+	2.74×10^{-5}	2.74×10^{-5}	2.74×10^{-5}	2.74×10^{-5}	2.74×10^{-5}	2.74×10^{-5}	2.74×10^{-5}
Ca^{2+}	5.00×10^{-6}	5.00×10^{-6}	5.00×10^{-6}	5.00×10^{-6}	5.00×10^{-6}	3.12×10^{-4}	3.19×10^{-4}
Al^{3+}	1.00×10^{-10}	9.25×10^{-7}	9.25×10^{-7}	1.79×10^{-9}	9.28×10^{-11}	1.52×10^{-8}	8.94×10^{-6}
$SiO_2(aq)$	1.00×10^{-6}	1.00×10^{-6}	5.68×10^{-5}	5.68×10^{-5}	5.96×10^{-4}	6.00×10^{-4}	1.72×10^{-3}
HCO_3^-	3.43×10^{-4}	3.43×10^{-4}	3.43×10^{-4}	3.43×10^{-4}	3.43×10^{-4}	3.43×10^{-4}	3.43×10^{-4}
F^-	1.00×10^{-10}	1.00×10^{-10}	1.00×10^{-10}	1.00×10^{-10}	1.00×10^{-10}	6.13×10^{-4}	6.28×10^{-4}
Cl^-	9.50×10^{-5}	9.50×10^{-5}	9.50×10^{-5}	9.50×10^{-5}	9.50×10^{-5}	9.50×10^{-5}	9.50×10^{-5}
				aqueous complexes			
$AlOH^{2+}$	1.51×10^{-11}	1.46×10^{-7}	1.46×10^{-7}	2.02×10^{-10}	6.80×10^{-14}	7.37×10^{-14}	5.34×10^{-12}
$Al(OH)_2^+$	2.38×10^{-12}	2.40×10^{-8}	2.40×10^{-8}	8.92×10^{-10}	2.96×10^{-12}	3.03×10^{-12}	2.58×10^{-11}
$Al(OH)_3(aq)$	4.10×10^{-14}	4.35×10^{-10}	4.35×10^{-10}	4.35×10^{-10}	1.44×10^{-11}	1.44×10^{-11}	1.44×10^{-11}
$Al(OH)_4^-$	7.50×10^{-16}	8.35×10^{-12}	8.35×10^{-12}	2.26×10^{-10}	7.54×10^{-11}	7.65×10^{-11}	8.92×10^{-12}
AlF_2^+	2.92×10^{-18}	2.67×10^{-14}	2.67×10^{-14}	1.35×10^{-18}	4.40×10^{-23}	1.64×10^{-9}	9.86×10^{-7}
$AlF_3(aq)$	3.59×10^{-24}	3.28×10^{-20}	3.28×10^{-20}	1.65×10^{-24}	5.31×10^{-29}	1.17×10^{-8}	6.91×10^{-6}
AlF_4^-	9.03×10^{-32}	8.23×10^{-28}	8.23×10^{-28}	4.14×10^{-32}	1.33×10^{-36}	1.79×10^{-9}	1.04×10^{-6}
$H_3SiO_4^-$	3.11×10^{-12}	3.27×10^{-12}	1.86×10^{-10}	5.04×10^{-9}	5.32×10^{-7}	5.44×10^{-7}	1.82×10^{-7}
CO_3^{2-}	3.00×10^{-12}	3.31×10^{-12}	3.31×10^{-12}	1.96×10^{-9}	7.03×10^{-8}	7.41×10^{-8}	2.81×10^{-9}
$CO_2(aq)$	3.40×10^{-4}	3.39×10^{-4}	3.39×10^{-4}	2.72×10^{-4}	9.46×10^{-5}	9.34×10^{-5}	2.61×10^{-4}
CaF^+	2.28×10^{-15}	2.28×10^{-15}	2.28×10^{-15}	2.25×10^{-15}	2.19×10^{-15}	7.77×10^{-7}	7.89×10^{-7}
$CaCO_3(aq)$	2.90×10^{-14}	3.19×10^{-14}	3.19×10^{-14}	1.84×10^{-11}	6.27×10^{-10}	3.56×10^{-8}	1.41×10^{-9}
				mineral modal abundances			
$\phi_{gibbsite}$		0.3751	9.9313×10^{-4}	0.	0.	0.	0.
$\phi_{kaolinite}$		0.	0.5826	0.	0.	0.	0.1500
$\phi_{k-feldspar}$		0.	0.	0.	0.4920	0.4934	0.6000
ϕ_{illite}		0.	0.	0.5491	0.3372	0.3366	0.1500
$\phi_{fluorite}$		0.	0.	0.	0.	4.9685×10^{-2}	5.0000×10^{-2}
ϕ		0.6249	0.4164	0.4509	0.1708	0.1204	5.0000×10^{-2}
v/v_0		7.876×10^{-8}	4.768×10^{-6}	2.985×10^{-5}	5.963×10^{-5}	1.514×10^{-4}	5.674×10^{-4}

adjusted for infiltration through a soil zone at the top of the weathered profile with the composition given in the column labeled inlet in table 1. The inlet concentration of the chloride ion is calculated by charge balance assuming values for the other species given in table 1 with an assumed pH of 4.3 and a log P_{CO_2} of −2. The unweathered host rock is represented as a homogeneous porous medium with the modal composition given in the column labeled zone 6 in table 1 consisting of minerals K-feldspar, illite (muscovite), kaolinite, and fluorite.

According to table 1 the pH jumps from its initial value of 4.3 to 5.75 across the gibbsite-kaolinite | illite reaction front as illite dissolves producing kaolinite and gibbsite. It jumps again to 6.75 across the illite | K-feldspar-illite reaction front as K-feldspar dissolves producing illite. The pH drops to approx 5.8 as the fluid comes to equilibrium with the hydrothermally altered phonolite host rock. The steep rise in the pH from approx 4.3 to 6.75 represents a hydrolytic front at which K-feldspar and illite dissolve, and kaolinite and gibbsite precipitate. The dominate aluminum species in the zones with fluoride present consist of the fluoride complexes AlF_3 and AlF_4^-.

Next the solution to the kinetic mass transport equations is considered. Kinetic calculations are based on the quasi-stationary state approximation taking into account kinetics of both mineral precipitation and dissolution reactions (Lichtner, 1988). Further details of the method of calculation may be found in Lichtner (1992). The kinetic rate constants and surface areas used in the calculation are listed in table 2. For K-feldspar the rate law is taken from Helgeson, Murphy, and Aagaard (1984). Illite is taken to have the same rate constant as K-feldspar but with a surface area 20 times smaller. A reference Darcy velocity of 1 m y^{-1} is used in the calculations.

Shown in figure 6 is the resulting volume fraction profile plotted as a function of distance for elapsed times of 2 my. Gibbsite along with secondary kaolinite and illite appear as alteration products during weathering as K-feldspar, fluorite, primary kaolinite, and illite dissolve. The qualitative features of the weathered profile and comparison with field observations are presented by Lichtner and Waber (1992). A thick, high porosity, kaolinite zone forms near the surface consisting of both primary and secondary kaolinite, followed by a dissolution front of primary kaolinite deeper in the profile. Both gibbsite and illite form bi-modal distributions. A plateau occurs in the K-feldspar profile with a gradual increase in modal abundance with depth approaching the value in the unweathered rock. The general features of these zones are in qualitative agreement with field observations.

Shown in figure 7A is the kinetic result for the mineral volume fractions corresponding to an elapsed time of 100,000 yrs plotted as a

TABLE 2

Kinetic rate constants k_m *and initial surface areas* s_m *used in the kinetic calculations*

Mineral	k (moles $cm^{-2}sec^{-1}$)	s (cm^{-1})
K-feldspar	3.16×10^{-16}	10.0
illite	3.16×10^{-16}	0.5
kaolinite	1.0×10^{-17}	45.0
gibbsite	$1. \times 10^{-16}$	5.0
fluorite	$1. \times 10^{-15}$	1.0